LL-37 fragments have antimicrobial activity against Staphylococcus epidermidis biofilms and wound healing potential in HaCaT cell line

Saporito, Paola; Mouritzen, Michelle Vang; Løbner-Olesen, Anders; Jenssen, Håvard

Published in:
Journal of Peptide Science

DOI:
10.1002/psc.3080

Publication date:
2018

Document Version
Peer reviewed version

Citation for published version (APA):
Saporito, P., Mouritzen, M. V., Løbner-Olesen, A., & Jenssen, H. (2018). LL-37 fragments have antimicrobial activity against Staphylococcus epidermidis biofilms and wound healing potential in HaCaT cell line. *Journal of Peptide Science*, *24*(7), Article 3080. https://doi.org/10.1002/psc.3080

LL-37 fragments have antimicrobial activity against Staphylococcus epidermidis biofilms and wound healing potential in HaCaT cell line

Journal:	*Journal of Peptide Science*
Manuscript ID	PSC-17-0147.R1
Wiley - Manuscript type:	Research Article
Date Submitted by the Author:	16-Feb-2018
Complete List of Authors:	Saporito, Paola; Roskilde Universitet, Science and Environment; Kobenhavns Universitet Biologisk Institut, Biology Vang, Michelle; Roskilde Universitet, Department of Science and Environment Løbner Olesen, Anders; Kobenhavns Universitet Biologisk Institut, Biology Jenssen, Håvard ; Roskilde University,
Keywords:	Human cathelicidin LL-37, S. epidermidis, Biofilm eradication, Wound healing

Peptides FK-12, KR-12 and VQ-12^{V26} derived from human LL-37 have antibiofilm properties. In addition, KR-12 and VQ-12^{V26} have wound healing potential and should be used as lead peptides for eradication of biofilms in catheters and infected wounds. Remarkably, in VQ-12^{V26} the single substitution aspartate to valine in position 26 leads to gain of antimicrobial function against *S. epidermidis* biofilms and enhanced wound closure *in vitro*.

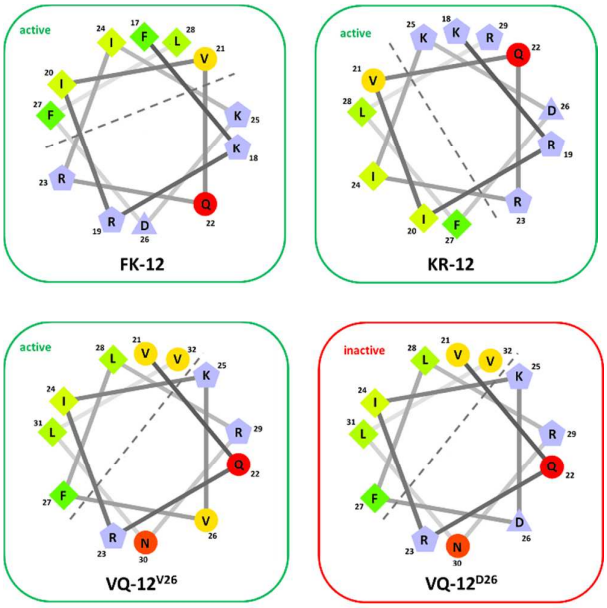

LL-37 fragments have antimicrobial activity against *Staphylococcus epidermidis* biofilms and wound healing potential in HaCaT cell line.

Saporito Paola, Vang Michelle, Løbner-Olesen Anders, Jenssen Håvard

Saporito Paola[a,b], Vang Michelle[b], Løbner-Olesen Anders[a], Jenssen Håvard[b*].

LL-37 fragments have antimicrobial activity against *Staphylococcus epidermidis* biofilms and wound healing potential in HaCaT cell line

* Correspondence to Håvard Jenssen Department of Science and Environment, Roskilde University, Universitetsvej 1, Postboks 260, 4000 Roskilde, Denmark

[a] Section for Functional Genomics and Center for Bacterial Stress Response and Persistence, Department of Biology, University of Copenhagen, Copenhagen, Denmark

[b] Department of Science and Environment, Roskilde University, Roskilde, Denmark

ABSTRACT

Staphylococcus epidermidis is a common nosocomial pathogen able to form biofilms in indwelling devices, resulting in chronic infections which are refractory to antibiotics treatment. Staphylococcal biofilms are also associated with the delayed reepithelization and healing of chronic wounds. The human cathelicidin peptide LL-37 has been proven active against *S. epidermidis* biofilms *in vitro* and to promote wound healing. As previous studies have demonstrated that fragments of LL-37 could possess an equal antibacterial activity as the parent peptide, we tested whether shorter (12-mer) synthetic fragments of LL-37 maintained the anti-biofilm and/or immune modulating activity, aiming at the identification of essential regions within the LL-37 parent sequence. Three fragments of LL-37 displayed improved activity against *S. epidermidis* in terms of biofilm inhibition and eradication, a reduced cytotoxicity to human keratinocytes and erythrocytes. In addition, KR-12 and VQ-12^{V26} enhanced wound healing potential, relative to LL37. FK-12 and KR-12 are truncated version of the cathelicidin, previously reported as valid antimicrobials, whereas VQ-12^{V26} is a single substituted LL-37 fragment. Remarkably, the single substitution aspartic acid to valine in position 26 caused gain of antimicrobial function in the inactive VQ-12 fragment. The combination of anti-biofilm, wound healing potential and low cytotoxicity makes KR-12 and VQ-12^{V26} promising therapeutic agents and lead compounds for further improvement and understanding of anti-biofilm and wound healing properties.

Keywords: Human cathelicidin LL-37; S. epidermidis; Biofilm eradication; Wound healing

INTRODUCTION

The excessive use of antibiotics in human and veterinary medicine, as well as agriculture, harms the community in the long term [**1-5**]. In fact, the misuse of antibiotics accelerates the natural-occurring mutation-driven antimicrobial resistance by selecting notsusceptible bacteria which can then spread vertically or horizontally [**6**]. Multidrug resistant bacteria or superbugs are now commonly found and impact both in and outside of hospitals and retirement homes. The scientific community is therefore pressured to find new and more effective drugs to halt this treat.

A promising alternative to antibiotics resides in the broad-spectrum and evolutionarily-conserved antimicrobial peptides (AMPs), or host defense peptides which may work as effectors of the immune response triggered in eukaryotes, upon infection by microbial agents [**7, 8**]. AMPs are generally short (10- 50 amino acids) and characterized by an amphiphilic configuration, derived from the presence of cationic residues on one side of the peptide and hydrophobic residues on the opposite side [**9**]. The amphipathic nature of AMPs allows them to interact with negatively-charged bacterial membranes and perturb the membrane bilayer, promoting either cell lysis, upon membrane disruption, or inhibition of intracellular processes such as nucleic acids and proteins synthesis [**10,11**].

Humans express a variety of AMPs, grouped into three major classes, namely cathelicidin, defensins and histatins which differ in structure and residue composition [**12**]. There is one unique human cathelicidin gene, transcribed as the pro-peptide hCAP18 and released as the active cathelicidin peptide LL-37, upon digestion by serine proteases [**13**]. LL-37 has pleiotropic activities both on pathogens and host cells: it is able to form pores through bacterial membranes, thus exerting an antimicrobial effect, while it also is modulating defense mechanisms [**14**]. Furthermore,

LL-37 has been demonstrated to have a positive effect on wound healing, both *in vitro* and *in vivo*, by increasing angiogenesis [**15**], re-epithelization [**16**], and chemotaxis [**17**]. The skin constitutes the first line of defense to the human body, and is itself shielded by pathogen bacterial colonization, thanks to the constitutive expression of low-levels of LL-37 by keratinocytes. Once the epithelial barrier fails due to infection or injury, the rate of LL-37 expression is further increased through the active synthesis by keratinocytes themselves and by the recruited immune cells such as neutrophil and mast cells. The increased levels of LL-37 halt bacterial proliferation while promoting re-epithelialization of the skin [**18**].

At the same time, the skin constitutes an optimal niche for a diversified microbiota, comprising the opportunistic pathogen *S. epidermidis*, which normally grows as a commensal but can turn pathogenic in immunocompromised patients when the epidermal barrier is breached [**19,20**]. A beneficial effect of *S. epidermidis* is its ability to prevent an excessive inflammatory response during re-epithelialization of damaged skin. This results from the *S. epidermidis* lipothecoic acid interaction with Toll-like receptor 2 on keratinocytes, which in turn prevents the release of the pro-inflammatory cytokine TNF-α [**19**]. *S. epidermidis* can penetrate the ulcerated epidermidis to reach the bloodstream and it is the most common cause of primary bacteremia and infection of indwelling medical devices, particularly in immunocompromised individuals and neonates [**21**]. *S. epidermidis* infections are increasingly resistant to antibiotics such as penicillins, aminoglycosides and quinolones [**22**]. *S. epidermidis* causes the onset of chronic infections, due to its ability to escape host defense mechanisms [**22,23**].

Both these characteristics of *S. epidermidis* infections relate to the pathogenic species ability to attach to solid surfaces and form a social community called biofilm, where bacteria are embedded into a self-secreted matrix composed mainly by exopolymers and DNA. The biofilm confers a protective niche to the bacteria and provides the bacterial population a reservoir of pathogens, thus enabling the persistence of the infection [**23**].

In particular, the naturally occurring antimicrobial peptide LL-37 has been proven effective in inhibiting biofilm formation [**24, 25**]. LL-37 is active against *S. epidermidis*: it is constitutively expressed in the skin of the newborn, where it helps maintaining the microbiota by inhibiting *S. epidermidis* growth [**23**].

A common approach in drug design is to make derivatives of natural products. Because, natural and synthetic AMPs constitute a promising alternative to antibiotics, we assessed the antimicrobial effect of truncated versions of LL-37 peptide against *S. epidermidis* and evaluated their efficacy as biofilm inhibitors or eradicators in comparison to the parent peptide. The aim was to identify the minimal sequence needed for activity, while aiming at reducing the cost and improving the ease of production of a lead compound useful for further design and activity improvement.

Therefore, we decided to scan the LL-37 sequence, by testing different fragments with a fixed length of 12 mer. The definite length of 12-mer was previously used as bioinformatic descriptor to identify active antimicrobials peptides derived from bactenecin [**26**]. Moreover, previous studies have tested the activity of 12 mer long fragments of LL-37, namely fragment KR-12, identified as a α-helix peptide, bearing the minimal antimicrobial sequence against *E. coli* [**11**] (Wang G., 2008) and fragment LL-12, proven to be antimicrobial inactive [**27**]. Those fragments were among the ones tested in our study.

In addition, the fragments ability to induce migration, a crucial aspect for wound healing, was tested. Cytotoxicity of the fragments and their parent peptide LL-37 was assessed in human keratinocytes and erythrocytes, respectively via lactate dehydrogenase release and hemolysis assay. Here we demonstrate that three LL-37 fragments: FK-12, KR-12 and VQ-12^{V26} have an improved activity against *S. epidermidis* in terms of biofilm inhibition and eradication, have a reduced cytotoxicity to human keratinocytes and erythrocytes. In addition, KR-12 and VQ-12^{V26} enhance keratinocytes migration more than the parent peptide.

LL-37 derived peptides inhibit growth of planktonic *S. epidermidis.*

To test the antimicrobial potential of LL-37 derived peptides against planktonic *S. epidermidis*, the minimal inhibitory concentration (MIC) for selected peptides was determined (Table 1). The parent peptide LL-37 was more potent than most of the fragments, with just FK-12, KR-12 and VQ-12^{V26} being equal to the parent peptide.

Furthermore, the minimal biocidal concentrations (MBC) were determined for LL-37, FK-12, KR-12 and VQ-12^{V26}. The lowest concentrations revealing no bacteria growth on the solid medium were reported as the MBC values (Table 2). The observed MBC values matched with the 48 hours MIC values (data not shown). If the MIC/MBC was reported below 4, the action of all the compounds at the MIC value was inferred to as being bactericidal.

Sequence-activity relationship analysis

The simple alignment of the best acting fragments sequences did not allow the identification of a minimal sequence needed for antimicrobial activity, as no residue was strictly needed for the antimicrobial activity (Table 3). Splitting LL-37 in four similar size fragments composed of residues 1-12 (LL-12), 9-20 (SK-12), 21-32 (VQ-12) and 26-37 (DF-12) creates four inactive peptides.

The only antimicrobial peptides FK-12 and KR-12 share overlapping residues 18-28, however the deletion or addition of any of these residues had no real contribution to the overall activity, as the comparison to the partly overlapping peptides SK-12 and VQ-12 showed (Table 3).

Remarkably, the substitution of aspartic acid to valine in position 26 resulted in a drop in the MIC values for VQ-12^{V26} and VQ-12 (Table 1). The substitution aspartic acid to valine increased both the charge and hydrophobicity of the resulting peptide and affected the peptide bioactivity. This

suggests that the overall physicochemical properties, rather than the sequence itself, are the main determinants for anti-biofilm activity.

LL-37 derived peptides inhibit *S. epidermidis* biofilm formation *in vitro*

The antimicrobial properties of the LL-37 fragments were further investigated by focusing on their inhibitory potential on *S. epidermidis* biofilm formation *in vitro*. This study was conducted by biofilm formation assay in polypropylene microtiter plates and was aimed at defining the essential residues for the previously reported antibiofilm properties of LL-37 [**23, 24**]. In a preliminary screening, all fragments were tested at a wider concentrations range (100-6.25 μg/ml) to select the best acting peptides and their optimal concentrations (Figure 1). The growth medium Mueller Hinton Broth (MHB) was used both as sterility control and to detect unspecific binding of the crystal violet dye to inorganic matter. The fragments FK-12, KR-12 and VQ-12^{V26} were the best biofilm inhibitors within the group, with the more pronounced anti-biofilm effects at the highest concentrations tested, which corresponded to their 2 x MIC values

The fragments FK-12, KR-12 and VQ-12^{V26} inhibit *S. epidermidis* biofilm formation

To compare the anti-biofilm activities of LL-37 and its fragments FK-12, KR-12 and VQ-12^{V26}, all these peptides were used at concentrations ranging from 100 to 12.5 μg/ml and tested for their *S. epidermidis* biofilm inhibition properties. The anti-biofilm activities of fragments FK-12, KR-12 and VQ-12^{V26} were higher than that of LL-37, reducing biofilm biomass by more than 80%. In fact, the peptides FK-12, KR-12 and VQ-12^{V26} inhibited biofilm formation at the 100, 50 and 25 μg/ml concentrations (Figure 2). FK-12 slightly inhibited biofilm formation also at 12.5 μg/ml concentration whereas KR-12 and, to a less extent also VQ-12^{V26}, promoted biofilm formation at

the same concentration. At the tested concentrations, LL-37 had a minimal impact on *S. epidermidis* biofilm: besides having a slight inhibitory effect at sub-MIC concentrations (25 and 12.5 μg/ml), it had clearly no effect at higher concentrations and apparently it had even a pro-biofilm effect at 50 μg/ml.

LL-37 derived peptides eradicate *S. epidermidis* biofilms *in vitro*

To investigate whether the antimicrobial effect observed for FK-12, KR-12 and VQ-12^{V26} was directed against bacteria in the biofilm rather than in the planktonic state, a biofilm eradication assay was performed on 1-day-old *S. epidermidis* biofilm. In a similar assay, all the not-adhering planktonic cells are removed from the wells by aspiration and repeated washing steps. Therefore, any observed effect is directed against biofilm embedded cells or biofilm structural components.

While the parent peptide LL-37 proved inactive against preformed *S. epidermidis* biofilms, a clear anti-biofilm effect was observed for the FK-12, KR-12 and VQ-12^{V26} fragments at their 2 × MIC concentration. In particular, the fragment FK-12 was the strongest eradicator, capable of removing 80% of the formed biofilm (Figure 3).

LL-37 derived peptides have low cytotoxicity

To evaluate the effect of FK-12, KR-12, VQ-12^{V26} and LL-37 on the host cells, primary cultures of human erythrocytes and the human keratinocytes cell line HaCaT were challenged with the peptides. To allow for correlation to the antimicrobial assays, equivalent concentrations and administration times were used. *In vitro* cytotoxicity was assessed by lactate dehydrogenase (LDH) release assay in the HaCaT cell line and by hemolysis assay in erythrocytes. The fragments FK-12, KR-12 and VQ-12^{V26} were clearly less toxic to human erythrocytes and keratinocytes than their parent peptide LL-37. In fact, at 100 μg/ml, the percent of cytotoxicity to HaCaT cells was above 30% for LL-37 and below 10% for FK-12, KR-12, VQ-12^{V26}, with the peptide KR-12 being the less

toxic of the three fragments. At 50 μg/ml, the cytotoxicity of LL-37 was slightly above 10%, whereas all the three fragments were not cytotoxic (Figure 4). Likewise, the parent peptide LL-37 was more cytotoxic to human erythrocytes than its fragments: at all the concentrations tested the percent of hemolysis was close to 0 for FK-12, KR-12, VQ-12^{V26}, whereas for LL-37 the percent of hemolysis was above 20% at 100 μg/ml and decreased for decreasing concentrations. Remarkably, at the lowest concentration of 6.25 μg/ml, the hemolysis induced by LL-37 was still higher than the one observed upon administration of the fragments FK-12, KR-12, VQ-12^{V26} at the concentration of 100 μg/ml. (Figure 5). Both these cytotoxicity data, taken together with the antimicrobial activity, demonstrated that the fragments have a better selectivity toward pathogens than the parent peptide (Table 4). In addition, the results suggested that neither topical nor systemic administrations of the fragments would be harmful to the recipient.

LL-37 derived peptides have wound healing potential.

Since LL-37 was previously reported to promote wound healing both *in vitro* and *in vivo*, the wound healing properties of the set of peptides used in this study were assessed in an *in vitro* scratch assay in HaCaT cells. All fragments were tested at 25 μg/ml concentrations, which correspond to a quarter of their MIC values, and epidermal growth factor was used as positive control, as previously described [**28**]. Shortly, the epidermal growth factor binds to the epidermal growth factor receptor, which stimulates the mitogen-activated protein kinase (MAPK) pathway resulting in increased migration of keratinocytes [**29, 30**]. LL-37 promotes keratinocytes migration by epidermal growth factor receptor transactivation and STAT3 phosphorylation [**31**]. Remarkably, all the fragments had a stronger effect than the parent LL-37 peptide (Figure 6). The LL-37 fragments were not cytotoxic to epithelial cells, but in addition showed wound healing potential, with the highest percent of wound closure observed for fragments KR-12, VQ-12, VQ-12^{V26} and IK-12, allowing us to infer that the wound healing activity should rely on the C-terminal half of the

parent peptide. Furthermore, and in contrast to what observed for their antimicrobial potential, VQ-12 and VQ-12^{V26} had a similar effect, thus suggesting that the residue in position 26 has not major impact on this activity.

The combination of antimicrobial and wound healing properties, together with low cytotoxicity, makes peptides KR-12, VQ-12^{V26} valuable as putative drugs for management of *S.epidermidis* infections in human skin.

CD spectra analysis

Circular dichroism (CD) analysis was performed to monitor the conformational changes of the set of peptides in water, water-2'2'2'trifluoroethanol (TFE) (1:4) and 20 mM SDS The peptide LL-37 itself is reported to be unstructured in pure water and to adopt α-helical secondary structure when bound to lipid bilayer surfaces [**11**]. All the peptides were likewise unstructured in water and adopted an α-helical conformation in water-TFE with the sole exception of peptides SK-12, IK-12 and DF-12 (Figure 7). The inability to assume a helical conformation in TFE, an isotropic solvent that mimics membrane environment, could be the reason of lack of antimicrobial activity for these peptides. However, since both the fragments VQ-12^{V26} and VQ-12 were able to adopt the same conformation but were not equally potent antimicrobials, the helicity alone does not account for the observed activity. Remarkably, in 20 mM SDS all the peptides adopted an α-helical conformation, except for the random-coil peptide DF-12 and the β-strand peptide VQ-12^{V26}. As the inactive peptide VQ-12 and its active variant VQ-12^{V26} adopted different secondary structures, the ability to form β-conformation could be the discriminant for the biological activity observed.

In silico analysis: physicochemical properties as predictive tools for bioactivity

Physicochemical properties have been computed for the parent peptide LL-37 and its fragments, by using chemo-informatics tool available on-line (ExPASy ProtParam) [**32**] In addition, a query on the antimicrobial peptide database (APD) [**33**] had further added some insights into the fragments properties, identified the already deposited LL-37 fragment KR-12 and enabled the prediction of its antimicrobial activities (Table 5).

The physicochemical properties of the peptides and their bioactivity indicators were used to predict, confirm and interpret the experimental results. As a general rule, AMPs are expected to have molecular weight (Mw) < 10 kDa, isoelectric point (pI) ≥ 10, net charge≥ 2, Hydrophobicity index (HI) > 0.5 (using Eisenberg scale) and instability index (II) < 40. Furthermore, transmembrane peptides have mean hydrophobicity (mH) < 0.2, hydrophobic peptides have positive GRAVY values and negative- or close to 0- Boman indices (BI) [**34**].

Due to their short length, all the tested peptides fell in the optimal range value for their Mw. Remarkably, all of them but DF-12 had optimal values of stability index, net charge and isoelectric point. Therefore, its lack of activity was consistent with the predictions. FK-12, KR-12 and LL-37 had a hydrophobic index mH> 0.5, thus fitting in the AMP predictor values. In contrast, both the active peptide for VQ-12^{V26} and its inactive counterpart VQ-12, had mH< 0.5. Therefore, this single parameter did not allow to discriminate between active and inactive fragments. An alternative hydrophobicity parameter, the hydrophobic moment μH, measures the separation of polar and nonpolar amino acids along the peptide axis and it predicts the potential of helix formation for a given peptide. The ADP database gave a helix pattern for any input peptide sequence. As per the APD outputs, the FR-12 fragment might form an α-helix and it had at least 5 hydrophobic residues on the same surface. It might interact with membranes and was predicted to be antimicrobial. The same prediction of membrane interaction potential and antimicrobial activity was given for both the biofilm active VQ-12^{V26} and biofilm inactive peptide VQ-12, both carrying 4 hydrophobic residues. In contrast, the biofilm inactive peptides DF-12 and IK-12 were predicted to be not antimicrobial as

they do not have hydrophobic residues on the same surface and cannot form an α-helix long enough to be considered antimicrobial. Therefore, when we compared the ADP database outputs with our experimental results, the ADP prediction tool gave both false negative and false positive results. A probable explanation is that the μH is a poor predictor of helicity in the bound state, since the helix formation would depend by helix-stabilizing side chain interactions. It has been proved that peptides with the same hydrophobic moment have a differential binding affinity to the membranes and that the sequence, rather than amino acids composition, has a major impact on the actual helix formation [**28**]. Moreover, all the listed peptides had negative GRAVY values and positive Boman indices.

Discussion

Human cathelidicin LL-37 is secreted in the skin where it acts as a natural AMP, able to halt the proliferation of a plethora of pathogens by forming pores across bacterial membranes. *S. epidermidis* is human skin commensal which can turn pathogenic in immunocompromised patients and is able to form biofilm. Preliminary data have shown that LL-37 inhibits *S. epidermidis* biofilm *in vitro* [**23**]. Our study aimed at identifying the minimal sequences needed for the antimicrobial and anti-biofilm properties of the LL-37 peptide by testing the biological activities of LL-37 scrambled fragments and comparing them to those of the parent peptide. Antimicrobial properties were evaluated against bacteria in their planktonic state, via the MIC assay, and against biofilm via inhibition and eradication assays. The peptides FK-12, KR-12 and VQ-12^{V26} were the best antimicrobial agents within the group of fragments analyzed. Remarkably, all of them had MIC values equivalent or proximal to the parent peptide but appeared to be more efficient inhibitors and eradicators of *S.epidermidis* biofilms.

Besides, as FK-12 and KR-12 acted as inhibitory to biofilms even at concentrations below their MIC value, an additional explanation needs to be found. The death itself of some cells within the

bacterial population and their consequent lysis, mediated by autolysin E, would release extracellular DNA and promote biofilm assembling in the remaining subpopulation [**35**]. The hypothesis arises that the fragments and LL-37 would inhibit the biofilm formation by halting the programmed cell death of bacterial sub-populations which in turn acted as a trigger for biofilm assembly.

The LL-37 fragment KR-12 is registered in the antimicrobial peptide database (APD), with ID AP00608. It is described as an α-helix peptide with antimicrobial activity against E. coli K12 but not cytotoxic to human cells [**11**]. The cytotoxicity data are consistent with our data. NMR analysis of KR-12 in lipid micelles proved that this peptide forms an amphipathic helix with cationic side chains which, upon binding, promote the clustering of bacterial membranes phosphatidylglycerols, activating voltage dependent potassium channels and promoting signal transduction [**11**]. A similar mechanism would most likely be valid also for the closely related fragment FK-12, but a definite confirmation would require similar NMR analysis to be performed. In addition, the peptide FK-13, which contains an additional arginine to FK-12, is reported as toxic to human cells [**11**]. This is interesting, since the fragment FK-12 we studied is not toxic to human erythrocytes and keratinocytes. Therefore, the removal of a single arginine in position 29 would result in the loss of the peptide cytotoxicity against t human cells.

CD spectra analysis conducted in presence of the isotropic solvent TFE did not prove a direct correlation between peptides secondary structure and antimicrobial activity. In fact, while the peptides SK-12, IK-12 and DF-12 assumed a random coiled structure and were equally inactive as an antimicrobial, all the other peptides folded into α-helices but were differentially active against *S. epidermidis.* Therefore, the α-helical arrangement is not sufficient to predict and discriminate for antimicrobial potential of the tested peptides. In contrast, in presence of SDS, an environment which more closely mimics bacterial membranes, the active peptide VQ-12^{V26} adopted a β-strand conformation, whereas the inactive peptide VQ-12 was α-helical. Therefore, the different biological activity observed upon the substitution aspartate to valine could be associated to the different

secondary structure adopted by the peptides VQ-12 and VQ-12^{V26}. Aside from helicity, the comparison among the fragments and the parent peptide clearly demonstrates that the shorter the sequence the higher the antibiofilm effect, which most likely associates to the peptides ability to penetrate the cellular membrane or biofilm matrix.

In addition, besides the crystal violet staining enables a good estimate of biofilm mass, it is not informative on bacteria viability. Therefore, it is not possible to incontrovertibly define the peptides effect as being bactericidal or, rather, directed against biofilm matrix components.

Remarkably, the fragments FK-12, KR-12 and VQ-12^{V26} have a better selectivity ratio; lower toxicity to the host and improved potency against the pathogen, than the parent peptide (Table 4). It has been proposed that the pleiotropic functions of LL-37 are mapped on different regions of the peptide. The hydrophobic N-terminal$^{1-13}$ has been associated with oligomerization, hemolytic and chemotactic properties, the main antimicrobial properties reside within the middle-region$^{17-31}$, while the C-terminal$^{32-37}$ is involved in the LL-37 tetramer formation at physiological pH [**11**, **12**]. The LL-37 tetramer is maintained in zwitterionic membranes, as is the case of human erythrocytes membranes. Instead the LL-37 tetramer dissociates in anionic bacterial membranes where it binds lipopolysaccharide in Gram-negative or phosphatidylglicerols in Gram-positive bacteria, and forms a long amphipathic α-helix that inserts into and disrupts the bacterial membranes [**11**]. The lack of the LL-37 N-terminal region in the fragments may explain the reduced hemolytic activity observed, while elevated binding propensity to acidic bacteria phospholipids, as the antimicrobial domain is maintained within the fragments FK-12 and KR-12.

By substituting the aspartic acid residue in position 26 with a valine, it was possible to switch the inactive peptide VQ-12 into the potent biofilm inhibitor and eradicator VQ-12^{V26}. This substitution correlates with an increase in net charge (2+ to 3+), isoelectric point, aliphatic index and hydrophobic dipolar moment, whereas all the other physicochemical parameters are concomitantly decreased (Table 5). In addition, this substitution results in a different conformation which

correlates with the biological activity observed. Regarding the wound healing potential, fragments KR-12 and VQ-12^{V26} had an increased effect on migration, whereas LL-12 reduced the keratinocytes migration compared to the untreated control. As the highest percent of wound closure was obtained upon stimulation with fragments KR-12, VQ-12, VQ-12^{V26} and IK-12, the healing property most likely rely on the C-terminal half of the parent peptide. In contrast to what observed for their antimicrobial potential, VQ-12 and VQ-12^{V26} had a similar effect on wound closure, thus suggesting that the residue in position 26 has not major impact on this activity. We suggest to further assess this hypothesis and implement the antibiofilm properties by a rational drug design, using these peptides as lead compounds and test their eradication properties on yet more established biofilms and mixed species biofilms. The precise mechanism of interaction with the pathogen and the antimicrobial mode of action should be further investigated.

Conclusion

In this study, we assessed the antimicrobial effect of truncated versions of LL-37 peptide against *S. epidermidis* by testing their potential as biofilm inhibitors or eradicators in comparison to the parent peptide. The fragments FK-12, KR-12 and VQ-12^{V26} exhibited an increased antimicrobial effect compared to the parent peptide by inhibiting bacterial attachment, biofilm growth and disrupting established biofilms. In addition, fragments KR-12 and VQ-12^{V26} increased migration of HaCaT cells in an *in vitro* wound model. At the same time, they demonstrated a reduced cytotoxicity toward human erythrocytes and HaCaT cells. We propose to further investigate the effect of amino acids substitution in the peptides set used in this study. This warrant and extended SAR study to investigate correlation of peptide sequence and biological activity both against *S. epidermidis* biofilm and toward wound healing.

METHODS

Peptides used in the study

All human LL-37 variants peptides used in the study are 12 residues long and correspond to different, in some cases overlapping, fragments of the human cathelicidin peptide LL-37 and were purchased from GenScript. Two fragments have completely overlapping sequences, except for one single residue in position 26, which is either a valine or an aspartic acid (Table 1).

HaCaT cell line

The HaCaT cell line was kindly donated from David Gram Naym. The cells were grown in Dulbecco's modified eagle medium (DMEM) with glutamax (Thermofisher, 31966-021), 10% FBS (Gibco, 10270), 100 units/ml penicillin, and streptomycin (Sigma, P0781). The cells were sub-cultivated approximately every third day, by washing with PBS and trypsinizing (Sigma, Lot T3924).

Wound healing

Wound healing was assessed by a scratch assay performed in 48 wells where 7.5 $\times 10^4$/well cells were seeded and incubated 24 hours to reach 95% confluency. The following day, the wells were washed with PBS, scratched manually with a 200 µl pipet tip and stimulated with 25 µg/ml of peptides diluted in DMEM containing 2% FBS. Epidermal growth factor was used as positive control. The migration of the HaCaT cells were monitored with the optical camera system called oCelloScope (BioSense, Denmark) for 24 hours [**36**]. The oCelloScope used the software

UniExplorer (8.0.0.7144 (RL3). Closure of the scratch was calculated as a percentage for time 0 and 24 and compared to the untreated control.

Bacterial strain

Staphylococcus epidermidis (HJ 056) from our laboratory strains collection was obtained from Statens Serum Institut in Copenhagen, Denmark and verified as an *S. epidermidis* by sequencing of the *dnaN* gene. Frozen bacteria were streaked on Luria Bertani (LB) agar plates in sterile conditions and allowed to grow at 37°C for 18 hours, until uniform colonies were observed. Agar plates were stored in the refrigerator and used for a maximum of 14 days as reservoir of bacteria for the experiment replicates. For every assay, single colonies were transferred to MHB and maintained overnight at 37°C in constant agitation to allow bacterial replication.

MIC assay

The minimal inhibitory concentrations (MIC) for the tested compounds were determined according to the microtiter broth dilution method [**37**]. Briefly, bacteria cultures grown overnight in constant agitation at 37° C were diluted (1:50) in fresh growth medium and allowed to grow in the same conditions of temperature and shaking. Once the OD_{600} equals to 0.4, the bacterial culture was further diluted in fresh MHB (1:500) to obtain a final bacterial inoculum ranging between 2-8 $\times 10^5$ cfu/ml. Eventually, 90 µl of this bacterial suspension were inoculated per well in the microtiter plate, previously filled with 10 µl of serial dilutions of the test peptides, starting from an initial concentration equal to 10 times the intended one (to take into account the final 1:10 dilution in the bacterial suspension). Multiple wells were used as growth medium sterility control. An additional check of the sterility conditions, as well as of the real bacterial concentration seeded, was obtained by plating on agar a further 1:500 dilution of the inoculum. Both the microtiter and the agar plates

were placed in the incubator at 37 C for 18 hours. The MIC was determined as the peptide concentration giving no visible bacterial growth. The sterility of the working conditions was assessed by the uniformity of morphology of bacterial colonies and the inoculum concentration was confirmed by counting of the bacterial colonies. After MIC reading, plates were further incubated for 1 day and plate was read again after 48 hours.

MBC assay

Minimal biocidal concentrations (MBC) were determined by plating on solid MHB agar 100 µl of bacterial suspensions from the MIC plate assay wells corresponding to and above the MIC values. Plates were no growth was visible after 24 hours of incubation at 37°C were considered to correspond to the biocidal concentration.

Biofilm assay

Biofilm formation and staining were conducted according to the microtiter dish biofilm formation assay protocol [**38**] with minimal modifications relative to growing medium and solvent used for crystal violet dissolution. The experimental set-up differs in the inhibition and eradication assays, the assays will therefore be described separately.

Biofilm inhibition assay

96 wells microtiter plates were prepared the day of stimulation, by addition of 10 x peptide (10 µl/well), diluted from the stock solution into sterile milliQ water. The overnight bacterial culture was diluted 1:100 and 90 µl/well of this bacterial suspension were added to every well, except for

those used as MHB sterility control. As negative control, 90 µl/well of cell suspension were added to 10 µl of milliQ water.

Biofilm eradication assay

Overnight bacterial cultures were diluted 1:100 in fresh MHB and 100 µl/well of this bacterial suspension were added to every well, except for those used as MHB sterility control. After overnight incubation at 37°C, wells were washed 2 times with PBS, then the peptides diluted in MHB were added according to the intended testing dilutions. Plates were then incubated overnight at 37°C.

Biofilm staining with crystal violet

Once the challenge time elapsed, the wells were washed 2 times with PBS (150 µl/well) prior to staining the attached biofilm with crystal violet (125 µl/well) for 10 minutes on the bench. The unattached staining was removed by aspiration and washing with PBS. Eventually the stain was dissolved in ethanol 96% (200 µl/well) for 10 minutes before transferring 100 µl/well in a new flat bottom plate for reading absorbance at 595 nm.

Hemolysis assay

Briefly, donors blood was collected into Vacutainer EDTA coated tubes and centrifuged at 800 g for 10 minutes to isolate red blood cells which were washed twice with sterile saline (0.9 % NaCl) and then diluted to a concentration of 20% red blood cells in saline.

In sterile conditions, 96 well round bottom polypropylene microtiter plates were filled with 100 µl/well of serially two-fold saline-diluted concentrations of peptides. 1 % Triton X100 and 0.9 %

NaCl were used respectively as positive and negative controls of hemolysis. The plate was incubated for 24 hours at 37°C in 5% CO_2 atmosphere to assess ability of peptides to penetrate and disrupt red blood cells membrane, thus releasing the hemoglobin and red coloring the supernatant. The day after, the plate was centrifuged at 250 g for 5 minutes and 20 µl of the supernatant were transferred into flat bottomed polystyrene plates, prefilled with 100 µl of saline. Absorbance readings at 546 nm for the different treatments were blank subtracted and reported as percentage of the positive hemolysis control.

LDH assay on HaCaT cell line

LDH leakage from treated and untreated cells were determined on supernatants by using the CytoTox 96® Non-Radioactive Cytotoxicity Assay (Promega), following manufacturer's instructions. The absorbance is presented as percent of cytotoxicity (absorbance from lysed cells was set as 100%).

CD spectroscopy

Circular dichroism (CD) experiments were performed on a J-815 circular dichroism spectropolarimeter (Jasco). Far-UV CD spectra were recorded after five accumulations at 20°C, using a 1-mm path length quartz cell, between 280 and 190 nm at 100 nm/min with a band width of 1 nm. All peptides were analyzed in water, in TFE/water (4:1, v/v) and 20 mM SDS.

Statistical analysis

Data analysis was performed with Graphpad Prism 6, statistical significance was calculated with t-test by comparison to the untreated control (*: $P< 0.05$; **: $P < 0.01$; ***: $P < 0.001$).

References

1. Llor C, Bjerrum L. Antimicrobial resistance: risk associated with antibiotic overuse and initiatives to reduce the problem. Ther. Adv. Drug. Saf. 2014; 5(6): 229–241.
2. WHO European strategic action plan on antibiotic resistance 2011–2016.
3. Barton M.D. Antibiotic use in animal feed and its impact on human health. Nutr. Res. Rev. 2000; 13(2): 279–299.
4. Chang Q, Wang W, Regev-Yochay G, Lipsitch M, Hanage W.P. Antibiotics in agriculture and the risk to human health: how worried should we be? Evol. Appl. 2015; 8(3): 240–247.
5. Economou V, Gousia P. Agriculture and food animals as a source of antimicrobial-resistant bacteria. Infect. Drug. Resist. 2015; 8: 49–61.
6. Blair JM, Webber MA, Baylay AJ, Ogbolu DO, Piddock LJ. Molecular mechanisms of antibiotic resistance. Nat. Rev. Microbiol. 2015; 13(1): 42–51.
7. Baltzer SA, Brown MH. Antimicrobial Peptides – Promising Alternatives to Conventional Antibiotics. J. Mol. Microbiol. Biotechnol. 2011; 20: 228-235.
8. Jenssen H, Hamill P, Hancock RE. Peptide antimicrobial agents. Clin Microbiol Rev. 2006 Jul;19(3):491-511.
9. Hancock RE, Sahl HG. Antimicrobial and host-defense peptides as new anti-infective therapeutic strategies. Nat. Biotechnol. 2006; 24: 1551–1557.
10. Guilhelmelli F, Vilela N, Albuquerque P, Derengowski S, Silva-Pereira I, Kyaw CM. Antibiotic development challenges: the various mechanisms of action of antimicrobial peptides and of bacterial resistance. Front. Microbiol. 2013; 4: 353.
11. Wang G. Structures of human host defense cathelicidin LL-37 and its smallest antimicrobial peptide KR-12 in lipid micelles.J Biol Chem. 2008 283(47): 32637–32643.
12. Dürr UH, Sudheendra US, Ramamoorthy A. LL-37, the only human member of the cathelicidin family of antimicrobial peptides. Biochim. Biophys. Acta 2006; 1758 (9): 1408–25.

13. Xhindoli D, Pacor S, Benincasa M, Scocchi M, Gennaro R, Tossi A. The human cathelicidin LL-37 - A pore-forming antibacterial peptide and host-cell modulator. Biochim. Biophys. Acta 2016; 1858: 546.
14. Steinstraesser L, Hirsch T, Schulte M, Kueckelhaus M, Jacobsen F, Mersch EA, Stricker I, Afacan N, Jenssen H, Hancock RE, Kindrachuk J. Innate defense regulator peptide 1018 in wound healing and wound infection. PLoS One. 2012;7(8):e39373 Epub 2012 Aug6
15. Koczulla R, von Degenfeld G, Kupatt C, Krötz F, Zahler S, Gloe T, Issbrücker K, et al. An angiogenic role for the human peptide antibiotic LL-37/hCAP-18. J. Clin. Invest. 2003; 111(11): 1665–1672.
16. Carretero M, Escámez MJ, García M, Duarte B, Holguín A, Retamosa L, Jorcano JL, Del Río M, Larcher F. In vitro and in vivo wound healing-promoting activities of human cathelicidin LL-37 J. Invest. Dermatol. 2008; 128(1): 223–236.
17. Yang D, Chen Q, Schmidt AP, Anderson GM, Wang JM, Wooters J, Oppenheim JJ, Chertov O. LL-37, the neutrophil granule- and epithelial cell-derived cathelicidin, utilizes formyl peptide receptor-like 1 (FPRL1) as a receptor to chemoattract human peripheral blood neutrophils, monocytes, and T cells. J. Exp. Med. 2000; 192(7): 1069–1074.
18. Afshar M, Gallo RL. Innate immune defense system of the skin. Vet. Dermatol. 2013; 24: 32–39.
19. Cogen AL, Nizet V, Gallo RL. Skin microbiota: a source of disease or defence? Br. Jour. Dermatol. 2008; 158(3); 442–455.
20. Lai Y, Di Nardo A, Nakatsuji V, Leichtle A, Yang Y, Cogen AL, Wu ZR, *et al*. Commensal bacteria regulate Toll-like receptor 3–dependent inflammation after skin injury. Nat. med. 2009; 15 (12): 1377-1382.
21. Rupp ME. Clinical characteristics of infections in humans due to Staphylococcus epidermidis, Methods Mol. Biol. 2014; 1106: 1–16.
22. Grice EA, Segre JA. The skin microbiome. Nat. Rev. Microbiol. 2011; 9(4): 244–253.

23. Otto M. Staphylococcus epidermidis—the'accidental'pathogen. Nat. Rev. Microbiol. 2009; 7(8): 555-567.

24. Nelson A, Hultenby K, Hell E, Riedel HM, Brismar H, Flock JI, *et al*. Staphylococcus epidermidis isolated from newborn infants express pilus-like structures and are inhibited by the cathelicidin-derived antimicrobial peptide LL37. *Pediatr. Res.* 2009; 66:174–178.

25. Jacobsen AS, Jenssen H. Human cathelicidin LL-37 prevents bacterial biofilm formation, *Future Med. Chem.* 2012; 4(12): 1587–1599.

26. Jenssen H, Fjell CD, Cherkasov A, Hancock RE. QSAR modeling and computer-aided design of antimicrobial peptides. *J Pept Sci.* 2008; 14(1):110-4

27. Wu WKK, Wang G, Coffelt SB, Betancourt AM, Lee CW, Fan D, Wu K, Yu J, Sung JJY, Cho CH. Emerging Roles of the Host Defense Peptide LL-37 in Human Cancer and its Potential Therapeutic Applications. *Int. J. Cancer.* 2010; 127(8): 1741–1747.

28. Hell E, Giske CG, Nelson A, Römling U, Marchini G. Human cathelicidin peptide LL37 inhibits both attachment capability and biofilm formation of Staphylococcus epidermidis. *Lett. Appl. Microbiol.* 2010; 50(2): 211–215.

29. Peplow PV, Chatterjee MP. A review of the influence of growth factors and cytokines in in vitro human keratinocyte migration. *Cytokine.* 2013; 62: 1–21.

30. Haase I, Evans R, Pofahl R, Watt FM. Regulation of keratinocyte shape, migration and wound epithelialization by IGF-1- and EGF-dependent signalling pathways. J. Cell. Sci. 2003; 116(15): 3227–3238.

31. Tokumaru S, Sayama K, Shirakata Y, Komatsuzawa H, Ouhara K, Hanakawa Y et al. Induction of Keratinocyte Migration via Transactivation of the Epidermal Growth Factor Receptor by the Antimicrobial Peptide LL-37. J. Immunol. 2005; 175 (7): 4662-4668.

32. Gasteiger E, Hoogland C, Gattiker A, Duvaud S, Wilkins MR, Appel RD, Bairoch A. Protein Identification and Analysis Tools on the ExPASy Server. (In) John M. Walker (ed): The Proteomics Protocols Handbook, Humana Press (2005). pp. 571-607.

33. Wang G, Li X, Wang Z. APD3: the antimicrobial peptide database as a tool for research and education. Nucleic Acids Res. 2016; 44: 1087-1093.

34. Osorio D, Rondon-Villarreal V, Torres P. Peptides: A package for data mining of antimicrobial peptides. *R. J.* 2015 7(1): 4–14.

35. Cherry MA, Higgins SK, Melroy H, Lee HS, Pokorny A. Peptides with the same composition, hydrophobicity, and hydrophobic moment bind to phospholipid bilayers with different affinities. J. Phys. Chem. B. 2014; 118(43): 12462-12470.

36. Vang M, Jenssen H. Optimized scratch assay for test of migration in vitro with optical camera- article submitted.

37. Wiegand I, Hilpert K, Hancock RE. Agar and broth dilution methods to determine the minimal inhibitory concentration (MIC) of antimicrobial substances. Nat. Protoc. 2008; 3(2): 163–175.

38. O'Toole GA. Microtiter Dish Biofilm Formation Assay. *JoVE*. 2011; (47): 2437.

Tables

Table 1. List of peptides used in the study with indication of name, residues position, sequence and MIC values in *S. epidermidis*

Table 1.

Peptide	Residue	Sequence[a]	MIC [µg/ml] [b]
LL-37	1-37	LLGDFFRKSKEKIGKEFKRIVQRIKDFLRNLVPRTES	50
LL-12	1-12	LLGDFFRKSKEK	>100
SK-12	9-20	SKEKIGKEFKRI	>100
FK-12	17-28	FKRIVQRIKDFL	50
KR-12	18-29	KRIVQRIKDFLR	50
VQ-12^{V26}	21-32	VQRIKVFLRNLV	50
VQ-12	21-32	VQRIKDFLRNLV	>100
IK-12	24-35	IKDFLRNLVPRT	>100
DF-12	26-37	DFLRNLVPRTES	>100

[a] the C-terminus of all peptides is amidated
[b] average from three independent biological replicates

Table 2. MBC, MIC and MBC/MIC for LL-37, its derivative fragments FK-12, KR-12 and VQ-12^{V26}

Table 2.				
antimicrobial	**MBC [µg/ml] [a]**	**MIC [µg/ml] [a]**	**MBC/MIC**	**activity**
LL-37	100	50	2	bactericidal
FK-12	50	50	1	bactericidal
KR-12	50	50	1	bactericidal
VQ-12^{V26}	50	50	1	bactericidal

MBC, minimum bactericidal concentration
MIC, minimum inhibitory concentration

[a] average from three independent biological replicates

Table 3. Comparison by sequence alignment of active and inactive LL-37 fragments tested as *S.epidermidis* biofilm inhibitors and eradicators

Table 3.			
Effective against *S. epidermidis* biofilm		**Not effective against *S. epidermidis* biofilm**	
peptide	**sequence**	**peptide**	**sequence**
		LL-12	LLGDFFRKSKEK
FK-12	FKRIVQRIKDFL	SK-12	SKEKIGKEFKRI
KR-12	KRIVQRIKDFLR	IK-12	IKDFLRNLVPRT
VQ-12^{V26}	VQRIK<u>V</u>FLRNLV	VQ-12	VQRIK<u>D</u>FLRNLV
		DF-12	DFLRNLVPRTES

Table 4. Comparison of antimicrobial and hemolytic activity for the peptides used in this study

Table 4.			
peptide	**MIC [µg/ml] [a]**	**HE_{10} [µg/ml] [a]**	**S**
FK-12	50	>100	>2
KR-12	50	>100	>2
$VQ\text{-}12^{26V}$	50	>100	>2
LL-37	50	50	1

HE_{10}: concentration of antimicrobials causing 10% hemolysis
S: selectivity ratio calculated as ratio of HE_{10} and MIC concentrations

[a] average of three independent biological replicates

Table 5. Physicochemical properties of the LL-37 and LL-37 fragments used in the study.

Table 5.										
peptide	**Mw [Da][a]**	**pI[a]**	**q[a]**	**AI[a]**	**mH[b]**	**GRAVY[a]**	**f %[a]**	**WW H[c] [kcal/mol]**	**BI[c] [Kcal/mol]**	**II[a]**
LL-37	4493.3	10.61	+6	89.46	0.44	-0.724	35		2.99	23.34
LL-12	1467.7	9.70	+2	65.0	0.38	-0.933	33	3.79	2.81	2.88
LK-12	1462.7	10	+3	65	0.49	-1.375	25	7.2	3.36	9.66
FK-12	**1561.9**	**11.53**	**+3**	**121.67**	**0.68**	**- 0.1**	**50**	**2.04**	**2.53**	**3.37**
KR-12	**1570.9**	**12.21**	**+4**	**121.67**	**0.75**	**-0.708**	**41**	**ND**	**4.02**	**3.37**
VQ-12^{V26}	**1484.8**	**12.01**	**+3**	**170.00**	**0.47**	**-0.633**	**50**	**1.26**	**1.47**	**21.35**
VQ-12	1500.8	11.23	+2	145.83	0.43	-0.008	58	2.42	2.53	22.14
IK-12	1465.7	10.84	+2	121.67	0.40	-0.258	41	2.36	2.62	31.91
DL-12	1445.7	6.73	0	89.17	0.60	-0.667	58	3.83	3.42	71.08

Mw: molecular weight; *pI*: isoelectric point; *q*: net charge; *AI:* aliphatic index; *mH:* mean relative hydrophobic moment; *f%:* total hydrophobic ratio; *GRAVY:* Grand average of hydropathicity; *WW H:* Wimley-White whole-residue hydrophobicity; *BI:* Boman Index; *II:* instability index

[a] calculated with EXpasy Protparam.

[b] calculated with HydroMCalc using Eisenberg scale

[c] calculated with the ADP database Calculation and prediction tab

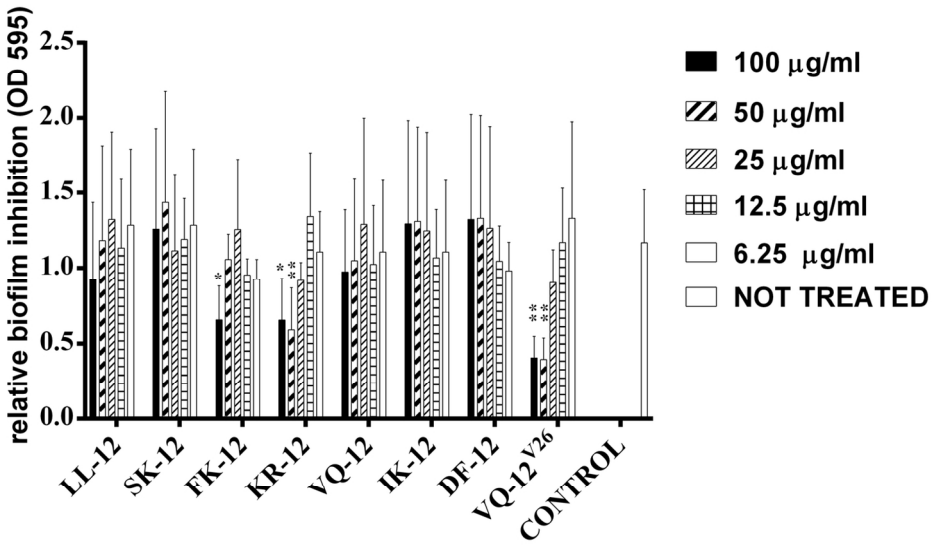

Figure 1. S. epidermidis Biofilm inhibition by LL-37 fragments, a preliminary screening. Diluted overnight cultures of S.epidermidis were challenged with the indicated concentrations of test peptides for 20 hours at 37° C in static conditions. The biofilms were stained with crystal violet and the biofilm mass was quantified by OD595 readings. Data represent the mean ± SEM of 2 biological replicate experiments, each consisting of 4 replicates. (*: P< 0,05: **: P < 0,01)

132x82mm (300 x 300 DPI)

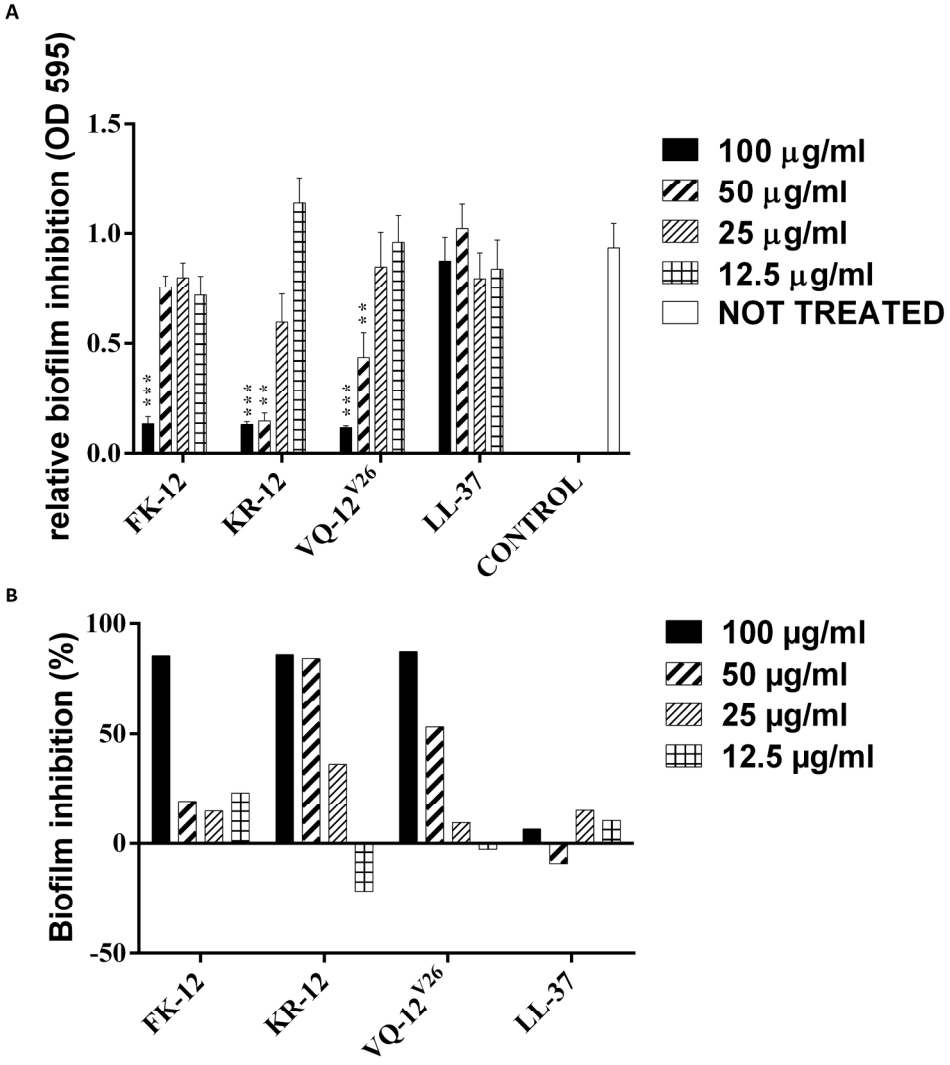

Fig 2. S.epidermidis biofilm inhibition. The biofilm inhibitory potential of the best acting LL-37 fragments was compared to the LL-37 peptide itself. Diluted overnight cultures of S. epidermidis were challenged with the indicated concentrations of test peptides for 20 hours at 37° C in static conditions. Data were plotted as stained biomass (A) and as percent of biofilm inhibition (B) versus peptides concentrations. Data represent the mean ± SEM of 2 biological replicate experiments, each consisting of 4 replicates. Statistical significance was calculated with t-test by comparison to the untreated control. (*: P< 0.05; **: P < 0.01; ***: P < 0.001). Data were plotted also as percentage of biofilm inhibition by normalizing the test compounds OD595 readouts to those of the negative control (untreated bacteria cells).

209x237mm (300 x 300 DPI)

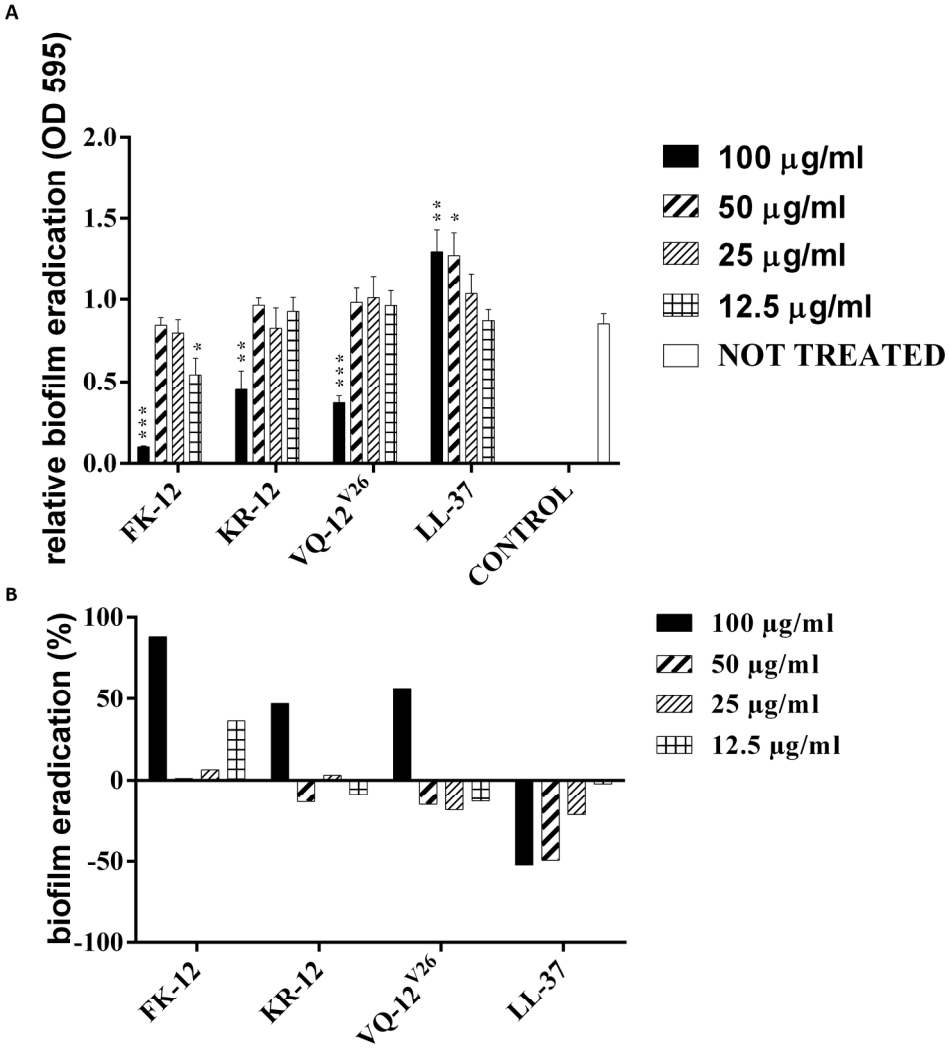

Figure 3. S.epidermidis biofilm eradication. The biofilm eradication potential of the best acting LL-37 fragments was compared to the LL-37 peptide itself. Data were plotted as stained biofilm biomass (A) and as percent of biofilm eradication (B) versus antimicrobials concentrations. Overnight cultures of S. epidermidis in MHB were diluted 1:100 in fresh MHB and plated in 96 well polypropylene plates (100 µl/well) and biofilm was allowed to form during overnight incubation at 37° C in static conditions. Fragments and LL-37 peptide were added to the S. epidermidis biofilm after removal of residual planktonic bacteria and allowed to react overnight. Data represented here are from 3 biological replicates, each consisting of 4 replicate wells (*: P< 0.05; **: P < 0.01; ***: P < 0.001).

209x235mm (300 x 300 DPI)

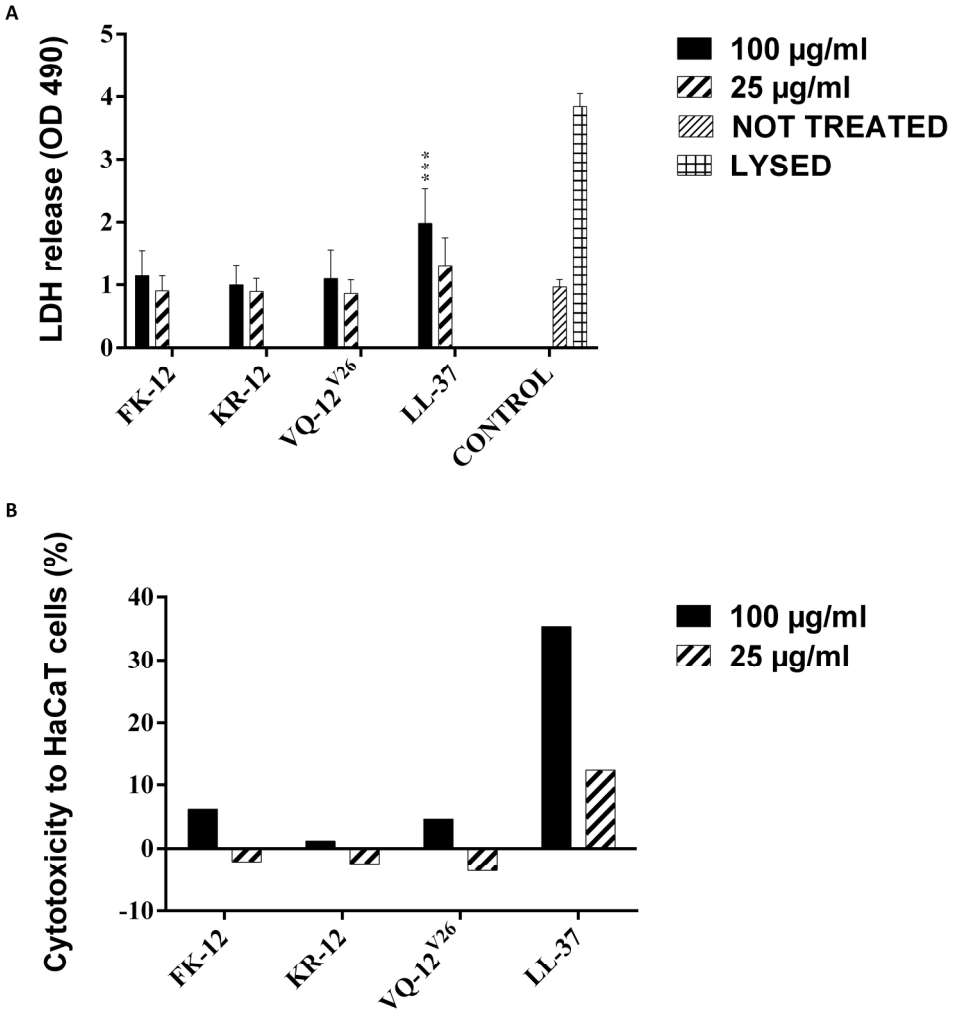

Figure 4. LDH release from HaCaT cells. HaCaT-1 cells (2 x 104 cells/well) were incubated in 96 wells micro-titer plates with antimicrobials at the tested concentrations overnight. The amount of LDH released was measured by OD490 readouts (A). Data were represented as percentage of toxicity (B) after baseline subtraction of untreated cells (negative control) and normalization to the lysed cells (positive control), whose absorbance was set as 100%. Data represented here are from 3 biological replicates, each consisting of 3 replicate wells. (*: P< 0.05; **: P < 0.01; ***: P < 0.001). The comparison to the untreated cells was not significant for all the fragments at the tested concentrations.

211x231mm (300 x 300 DPI)

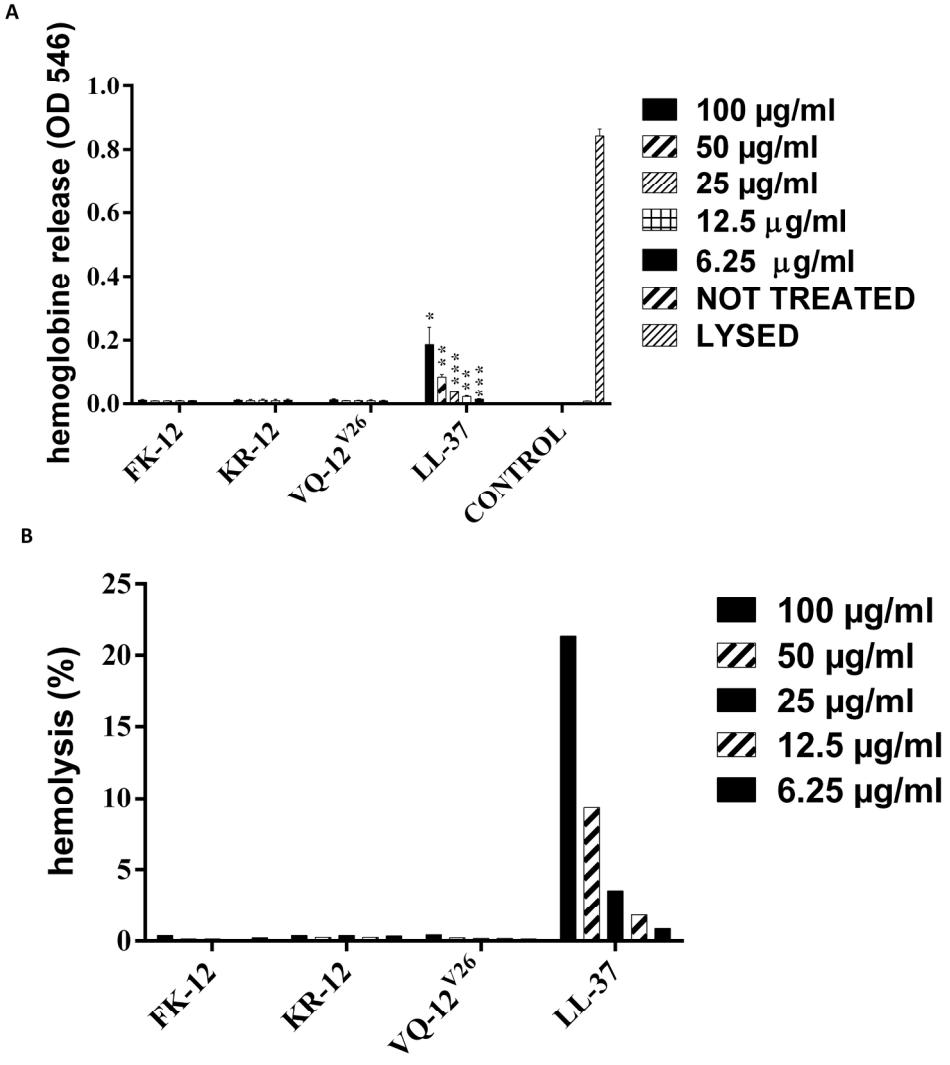

Figure 5. RBC hemolysis. The hemoglobin release from red blood cells upon overnight treatment with the test compounds was measured as OD546 readouts (A). Data are reported also as percent of hemolysis after normalization to the lysed cells (B). Data represented here represent mean ± SEM of triplicate experiments conducted on erythrocytes collected from different donors (*: P< 0.05; **: P < 0.01; ***: P < 0.001).

209x237mm (300 x 300 DPI)

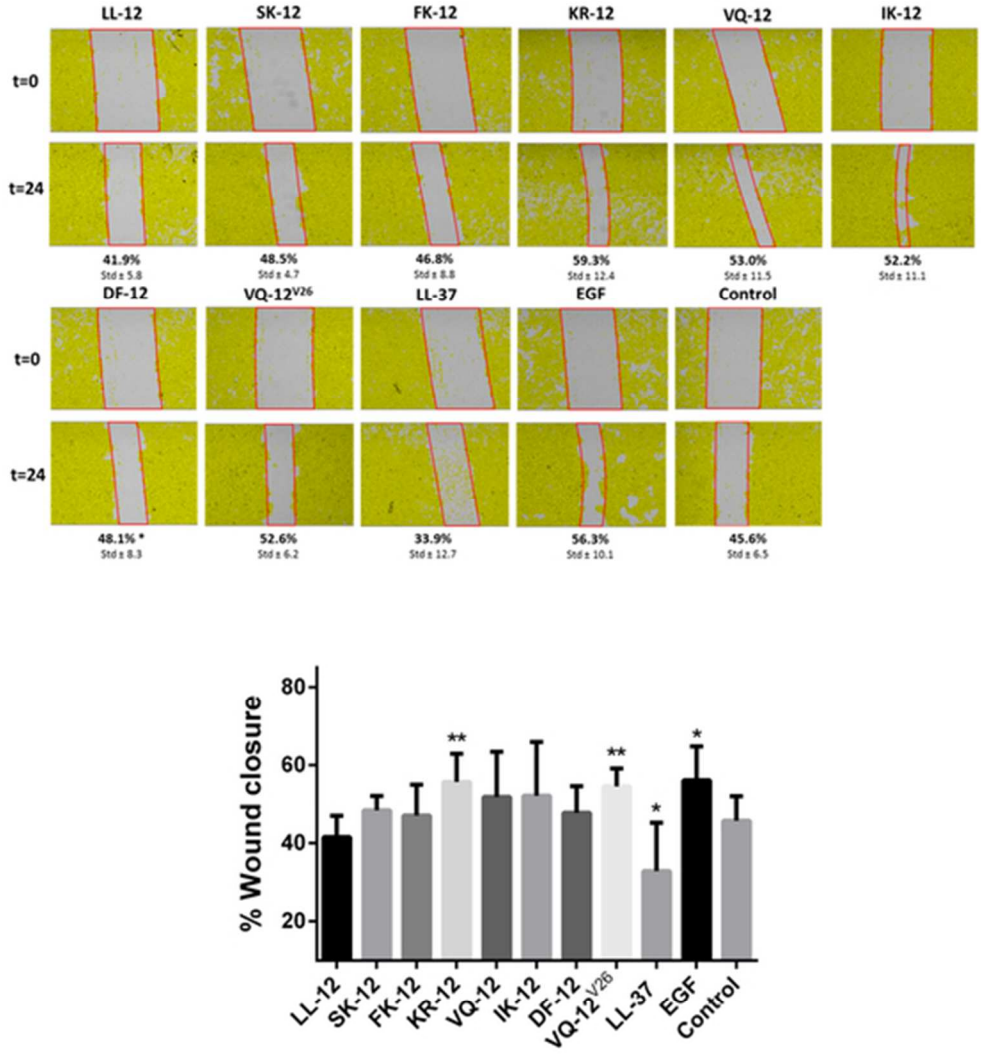

Figure 6. Migration of HaCaT cells as a result of LL-37 fragment treatment. The migration effect of LL-37 fragments were tested at 25 µg/ml concentration on HaCaT cells in low FBS in a scratch assay. The closure of the gap was measured every hour on an oCelloScope for 24 hours. Pictures of t=0 (top row) and t=24 (bottom row) taken by the oCelloScope (A)Data represent the average of three independent triplicates. Graphic representation of scratch assay (B) (*: P< 0.05; **: P < 0.01; ***: P < 0.001).

47x52mm (300 x 300 DPI)

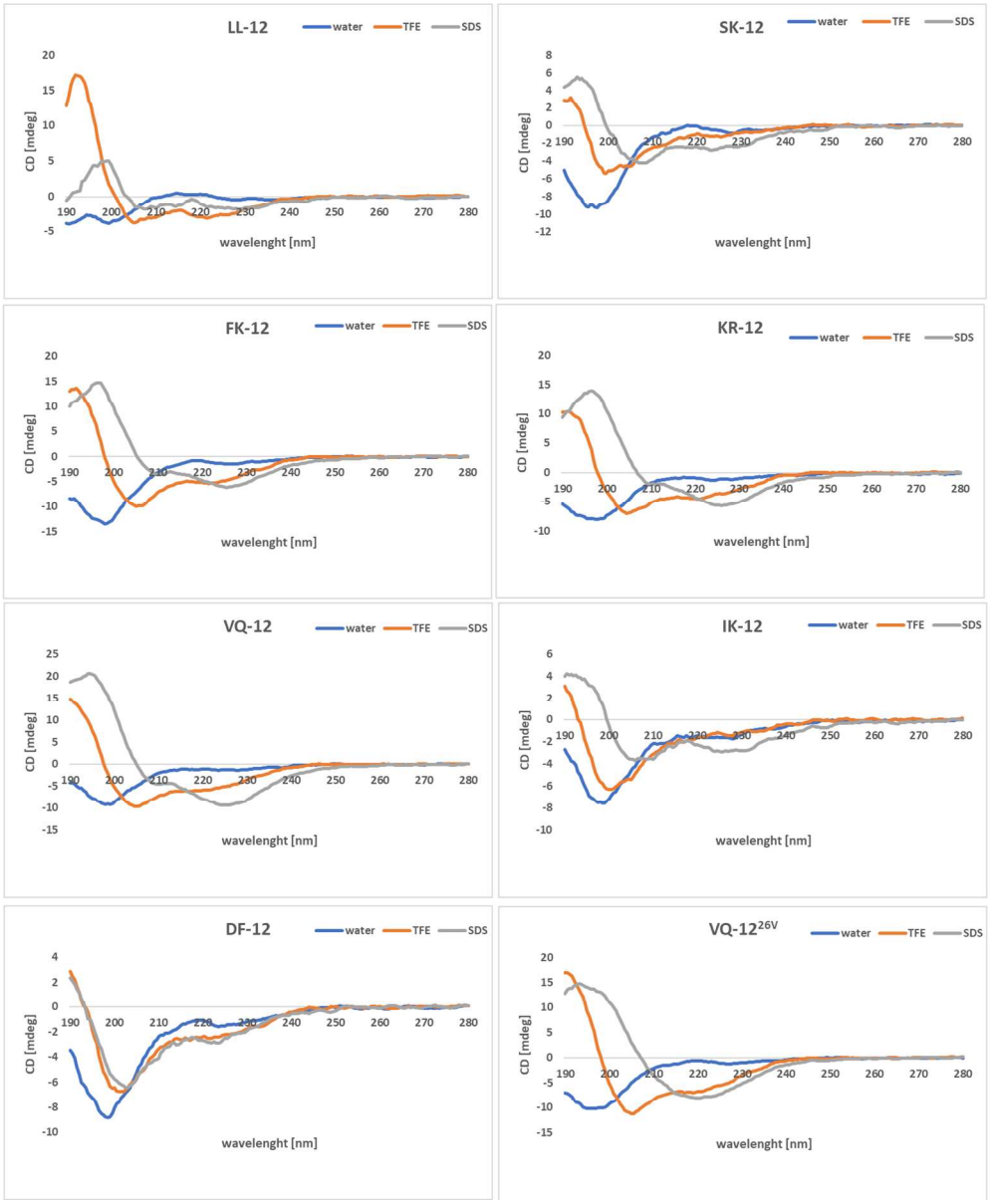

Figure 7. CD spectra analysis of the test peptides in water and TFE-water (4:1, v/v) Circular dichroism (CD) experiments were performed on a J-815 circular dichroism spectropolarimeter (Jasco). Far-UV CD spectra were recorded after five accumulations at 20°C, using a 1-mm path length quartz cell, between 280 and 190 nm at 100 nm/min with a band width of 1 nm. All peptides were analyzed in water, in TFE/water (4:1, v/v) and 20 mM SDS.

128x155mm (300 x 300 DPI)